IEEE Access
Multidisciplinary | Rapid Review | Open Access Journal

Received April 7, 2021, accepted April 25, 2021, date of publication April 30, 2021, date of current version May 10, 2021.

Digital Object Identifier 10.1109/ACCESS.2021.3076787

Low-Voltage Ride-Through Coordinated Control for PMSG Wind Turbines Using De-Loaded Operation

CHUNGHUN KIM[1], (Member, IEEE), AND WONHEE KIM[2], (Member, IEEE)
[1]Department of AI Electrical Engineering, Pai Chai University, Daejeon 35345, South Korea
[2]School of Energy Systems Engineering, Chung Ang University, Seoul 06974, South Korea

Corresponding author: Wonhee Kim (whkim79@cau.ac.kr)

This work was supported in part by the Energy Cloud Research and Development Program through the National Research Foundation of Korea (NRF) funded by the Ministry of Science, ICT under Grant NRF-2019M3F2A1073313 and in part by the Climate Change Response Technology Development Program through the NFR by the Ministry of Science, ICT under Grant NRF-2021M1A2A2065445.

ABSTRACT Low-voltage ride-through (LVRT) is important for the grid integration of wind power systems (WPSs). Each grid operator defines a grid code, including the LVRT requirement, considering their power system characteristics. During grid faults, LVRT is needed for the protection of WPS because the over current can induce damage to the power converter system. An important issue in the LVRT method of WPS is the energy capacity because sufficient reserve energy capacities of wind turbine inertia and an energy storage system (ESS) are needed for a successful LVRT operation. Although ESS can store excess energy of the WPS during a grid fault, it is physically limited considering its energy capacity. Moreover, WPS has a low reserve energy capacity, especially when the WPS operates in high wind speed conditions. Thus, we propose the deloaded operation of WPS for the preparation of LVRT by reducing the power generation of WPS. The effectiveness of the proposed method is validated by modeling a WT and an ESS topologically and performing simulations using the MATLAB/Simulink SimPowerSystems toolbox.

INDEX TERMS Deloaded control, DC link voltage, energy storage system, fuzzy-logic controller, rotor inertia, low-voltage ride-through, rotor speed limitation, pitch angle control.

NOMENCLATURE

- ESSs: Energy storage systems
- DFIG: Doubly-fed induction generator
- LVRT: Low-voltage ride-through
- MPPT: Maximum power point tracking
- MSC: Machine-side converter
- GSC: Grid-side converter
- PCC: Point of common coupling
- PI: Proportional-integral
- PMSG: Permanent magnet synchronous generator
- SoC: State-of-charge
- WP: Wind power
- WPS: Wind power system
- WTs: Wind turbines

I. INTRODUCTION

As more wind power is installed in power systems, grid integration methods become more important to protect both the power system and wind power system (WPS). Permanent magnet synchronous generator (PMSG) wind turbines (WTs) are widely used for this purpose as they offer better control responses than that of other WPSs. Although doubly fed induction generator (DFIG) WTs can be controlled using a power converter system, they have a lower control range compared to that of the PMSG WT because the former has a lower power capacity of power converter system. Thus, the major advantage of a PMSG WT is its large operation range because it fully uses power converters, that is, machine-side converters (MSCs) and grid-side converters (GSCs) [1], [2]. Therefore, we consider the control of PMSG WT for low-voltage ride-through (LVRT) by modulating the amount of power generation which is less than maximum available WP at a given wind speed [3] before a grid fault occurs.

WP integration issues become more important issue as the wind power (WP) proportion among entire power system capacity. There are many issues about WP integration in power system, however, the LVRT is one of the most important integration issue. LVRT is a control methodology to protect WPS and to remain connected to power system

The associate editor coordinating the review of this manuscript and approving it for publication was Yang Li.

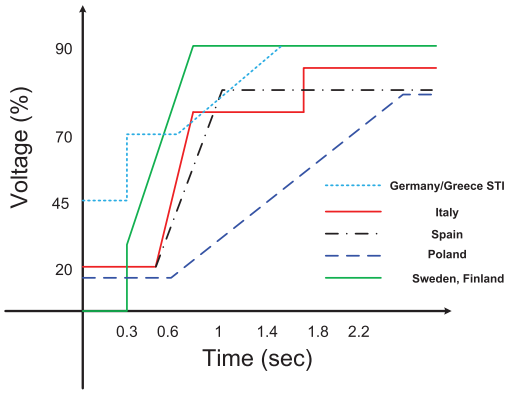

FIGURE 1. Limit curves for voltage to allow generator disconnection.

for stable operation of power system after the grid fault is cleared. During LVRT operation, WPS switch the control mode from maximum power point tracking (MPPT) control into low power production control mode. By reducing the power generation level, WPS can be protected from over current in power converter system and WPS can support power grid stability by producing reactive power to the grid during fault. Thus, the objective of reliable operation during grid fault is achieved from LVRT operation with reduced power generation which is different to MPPT control in normal operation condition [4], [5]. Each power system defines the reactive power support during grid fault in its grid code to support the grid voltage regulation [6]. Because of grid voltage reduction during the grid fault and current limit of the power converter system, WP should be controlled properly to protect the power converter system and produce reactive power to the grid. As shown in Fig. 1, grid operators have different requirement to WPS about LVRT and more advanced LVRT control method is required as WP penetration level is increased.

Several methods have been studied to improve the LVRT performance. A proportional-integral (PI) linear controller was introduced to regulate DC-link voltage for transient response. Details of performance comparisons considering unbalanced voltage fault was described in [7]. For better transient response, nonlinear dynamics were considered using feedback linearization in [8]. For further reduction in controller complexity, sliding mode control was introduced for effective consideration about nonlinear dynamics [9]. From this method, better transient response was guaranteed with robustness about the WPS parameters variations. A coordinated control of an MSC control and a pitch angle control without additional device was studied in [10]. However, extreme case with high wind speed was not included in this study. By switching functions of power converter systems, the MSC controls for DC-link voltage regulation and the GSC controls both of active and reactive power in [11], [12]. In [13], the asymmetrical grid fault was considered especially with the most serious fault condition. The DFIG was controlled to supply the positive-sequence reactive current to support the power grid. Other studies of LVRT controller using additional devices were introduced. In respect to energy efficiency during grid fault, energy storage systems (ESSs) are one of the best solution for LVRT. Since ESSs can be used various WPS applications besides LVRT, it can be considered there is no additional cost when using ESSs for LVRT [4]. By using ESSs with coordinated control of WPS, a more reliable and economic operation can be achieved. In [14], ESS is used for DC-link voltage regulation of WPS. In [15], [16], ESS controllers were designed for voltage at the point of common coupling (PCC) by supporting LVRT during grid fault. Reactive power control methodology of wind power plant was introduced in [17].

In this study, we propose a de-loaded operation for the LVRT of WPS during a grid fault. We analyze the reserve power of the WPS and ESS under certain wind conditions. Under high wind speed conditions, there is a low reserve power capacity in the WPS. If the ESS has sufficient reserve (charging) capacity under high wind speed conditions, it can result in reserve energy capacity issues during grid faults. Thus, by using wind speed and ESS state of charge (SoC) data, we obtain a proper de-loaded operation defined from the WP analysis. From the de-loaded operation, WPS can handle LVRT successfully without any energy capacity issues and minimize the reduction of power production. Compared to the previous work [18], the proposed method can effectively solve the problem due to the insufficient reserve energy of WPS and ESS for LVRT. We validated the effectiveness of the proposed method by performing simulations using the MATLAB/Simulink SimPowerSystems toolbox considering a topological circuit model. The simulation results show that the proposed method effectively achieves reliable operation without violating constraints. The benefits of the proposed method over previous fuzzy-based LVRT methods are as follows.

- The proposed method ensures successful LVRT control without any energy capacity limitation problem.
- The proposed method minimizes the power reduction involving the LVRT preparation.
- the proposed method can effectively solve the problem due to the insufficient reserve energy of WPS and ESS for LVRT.

II. PMSG WPS

In this section, the overall mechanical model of WTs is introduced. Moreover, mathematical model of the MSC and GSC of PMSG are described. Dynamic model of DC-link voltage is also introduced considering generation power and transferred grid power. Lastly, ESS model is introduced considering SoC and conventional linear controller for DC-link voltage regulation.

A. MECHANICAL POWER OF WTs

Using WT parameters, the mechanical power generation model of the WTs can be described. The WT parameters include the tip speed ratio λ, WT rotor speed ω_m, rotor radius R. Tip speed ratio can be described as following

equation using the WT parameters and a wind speed v_{wind}.

$$\lambda = \frac{\omega_m R}{v_{wind}}, \tag{1}$$

Since the wind speed is a given value, the tip speed ratio can be modulated by controlling rotor speed. The tip speed ratio and pitch angle β are main control variable and it defines the power coefficient of WT, C_p. A is a blade swept area. Maximum available WP can be obtained by controlling rotor speed properly according to given wind speed. That is, WT can produce maximum available power for given wind speed by maximizing power coefficient using rotor speed control. Following equation describes the mechanical power of WT [10].

$$P_t = \frac{1}{2}\rho A C_p(\lambda, \beta) v_{wind}^3, \tag{2}$$

where ρ is the air density. Thus, mechanical power of WT is controlled by rotor speed and pitch angle. Pitch angle is used only when reducing the wind power and rotor speed is controlled to modulate the WP to certain amount corresponding generation and grid condition. Rotor speed is indirectly controlled by power converter system such as the MSC. The difference between mechanical WP and electrical power transferred to the grid by the MSC.

B. MSC MODEL

One part of the mechanical power is transferred to electrical power grid by the MSC and the other part of the mechanical power is transferred to rotor inertia. Because of it, MSC model is important to control the WT and WP corresponding to various situations. That is, MSC control is very important for stability of both WT and power converter system, such as DC-link voltage. For LVRT, DC-link voltage regulation is the main issue to protect converter system. However, we propose the de-loaded control method which considers mechanical power by modulating rotor speed since some extreme case such as high wind speed can result in out of control. The MSC model can be described as following equation [12] including PMSG voltage, electrical torque, and rotor speed.

$$\begin{aligned} v_{dg} &= R_s i_{dg} + L_s \frac{di_{dg}}{dt} - \omega_s L_s i_{qg}, \\ v_{qg} &= R_s i_{qg} + L_s \frac{di_{qg}}{dt} + \omega_s L_s i_{qg} + \omega_s \lambda_f, \\ T_e &= \frac{3}{2} p \lambda_f i_{qg}, \\ T_m - T_e &= J \frac{d\omega_m}{dt}, \end{aligned} \tag{3}$$

where v_{dg} and v_{qg} are the stator DQ axis voltages. i_{dg} and i_{qg} are the stator currents of the PMSG. L_s and R_s are the stator inductance and resistance. ω_s denotes the electrical rotor flux speed. ω_m denotes the mechanical rotor speed. λ_f denotes the electrical rotor flux. p denotes pole pairs of the generator. T_e and T_m indicate the electromagnetic and mechanical torques, respectively. J denotes the rotor inertia. By using WP and torque of the WT, we can control the rotor speed of WT. There is energy buffer between WT and MSC, it is important to use this energy buffer according to various objectives such as MPPT and LVRT.

C. GSC MODEL

In WPS, the GSC mainly regulate the DC-link voltage and MSC power is transferred to the grid from this control method. The overall GSC model can be described by following equation [19].

$$\begin{aligned} v_d &= v_{id} - R i_d - L \frac{di_d}{dt} + \omega L i_q, \\ v_q &= v_{iq} - R i_q - L \frac{di_q}{dt} + \omega L i_d, \end{aligned} \tag{4}$$

where L and R are the grid side line inductance and resistance, respectively; v_d and v_q are the grid side DQ-axis voltages. i_d and i_q denote the grid side DQ-axis currents. v_{id} and v_{iq} denote the GSC DQ-axis voltages. We assume that the DQ-axis rotating reference frame is aligned with measured value of the grid voltage [19]. Following equation describes the active and reactive powers of the GSC.

$$\begin{aligned} P_{grid} &= \frac{3}{2} v_d i_d, \\ Q_{grid} &= \frac{3}{2} v_d i_q, \end{aligned} \tag{5}$$

where P_{grid} and Q_{grid} are the active and reactive powers, respectively.

D. DC-LINK VOLTAGE MODEL

For proper operation of the power converter systems such as the MSC and the GSC, it is important to regulate DC-link voltage even in grid fault situation [11]. Following equation describes DC-link voltage according to power relationship.

$$P_c = C V_{dc} \frac{dV_{dc}}{dt} = P_g - P_{grid}, \tag{6}$$

where P_g and P_{grid} denote the power of the MSC and GSC, respectively; P_c is the power transferred to the DC-link capacitor. C denotes the DC-link capacitor. V_{dc} denotes DC-link voltage. Since the DC-link voltage regulation is important for the MSC and GSC controls, one of these converters takes the role of the voltage regulation.

E. ESS MODEL

Nowadays, ESS is interconnected to WPS for several objectives. It can charge and discharge the energy for improving power quality, supporting grid stability and protecting WPS. For reliable operation of ESS, physical constraints such as SoC should be accounted. The SoC should be between 0 to 1 and it is better to have marginal stable region for better control performance. When the ESS interconnected with WPS, ESS is controlled for DC-link regulation and the power reference of the ESS can be defined by following equation.

$$P_{ESS}^* = K_P(V_{dc}^* - V_{dc}) + \int K_I(V_{dc}^* - V_{dc}) \tag{7}$$

P_{ESS}^* denotes the ESS power reference. To regulate the DC-link voltage, P_{ESS}^* is determined using the DC-link voltage error. This conventional control method of the ESS has a limitation when the ESS SoC reaches its maximum value as 1,

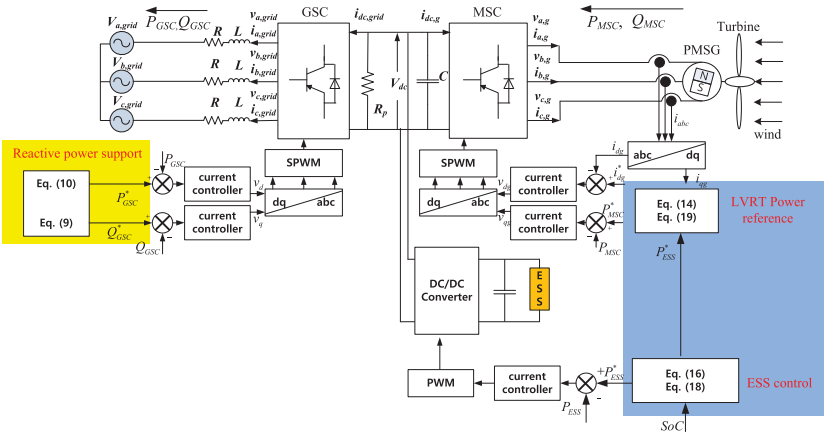

FIGURE 2. Overall control block diagram of the proposed method.

which can result in severe problem transient response. Thus, we considered de-loaded operation of WPS when coordinated with ESS control. We introduced this coordinated control considering WPS de-loaded control in the next section. In the proposed method, we used SoC value for evaluating reserve energy of the ESS. The SoC can be determined as following equation.

$$W_{ESS}(t) = \int_0^t P_{ESS}(u)du + W_{ESS}(0) \tag{8}$$

$$SoC(t) = W_{ESS}(t)/W_{Max} \tag{9}$$

W_{ESS} and W_{Max} denote the ESS energy and the maximum ESS energy capacity, respectively.

III. PROPOSED LVRT CONTROL SYSTEM

For stable operation during a grid fault, we proposed a de-loaded operation method with lower rotor speed than that of MPPT operation. From the de-loaded operation method, the reserve energy of rotor inertia is increased considering its maximum speed limit. Even though the de-loaded operation can be accomplished both with lower and higher rotor speed compared to the MPPT rotor speed, the proposed method utilizes lower rotor speed operation for more reserve energy from rotor inertia. The overall control structure is illustrated in Fig. 2. The current controllers are composed of inner and outer loop controller and the inner loop controllers are designed to have faster response compared to outer loop controllers for proper transient response. The control mode transition between no-fault and normal (MPPT) operation occurs when the grid voltage is reduced to less than 80% of its normal value.

A. GSC ACTIVE AND REACTIVE POWER REFERENCES

GSC controls active to regulate the DC-link voltage and reactive power to support the grid voltage restoration. In normal operation, GSC controls to regulate the DC-link power. However, GSC should focus on controlling the reactive power to support the grid voltage when the grid voltage fault and the requirement about reactive power is defined in grid code. When the grid voltage reduces to less than 50%, GSC should produce full reactive power current to the grid. Therefore, the DC-link voltage regulation performance could be poor. Thus, WPS needs improved LVRT control strategy to satisfy both grid requirement and WPS protection. The requirement about reactive power support during grid fault can be described as following equation.

$$\begin{aligned} I^*_{q,GSC} &= 2V_{sag}, \quad (\text{for } I^*_{q,GSC} \le 1 \text{ pu}) \\ Q^*_{GSC} &= I^*_{q,GSC} V_d, \end{aligned} \tag{10}$$

where $I^*_{q,GSC}$ indicates the reactive current reference corresponding to the grid voltage sag, V_{sag}. V_{sag} is a voltage difference between the normal grid voltage and reduced grid voltage due to the grid fault. It can be described as follows.

$$V_{sag} = V_{norm} - V_{fault} \tag{11}$$

Q^*_{GSC} denotes the reactive power reference, which is determined using $I^*_{q,GSC}$ and the grid d-axis voltage, V_d. As shown in Eq. 11, the GSC gives full reactive current when the grid voltage is less than 50% of normal value as grid codes require [6]. Since GSC should satisfy grid code requirement, reactive power reference is determined first according to the grid voltage at the grid fault. After that, GSC active power reference is determined according to the reactive power reference.

$$\begin{aligned} I^*_{d,GSC} &= \sqrt{1 - (I^*_{q,GSC})^2}, \\ P^*_{GSC} &= I^*_{d,GSC} V_d, \end{aligned} \tag{12}$$

where, $I^*_{d,GSC}$ is the active current reference. P^*_{GSC} denotes the active power reference.

B. MSC ACTIVE POWER REFERENCE

Since the GSC should focus on reactive power control during grid fault, the MSC should take the role of DC-link regulation coordinating with the ESS. Before determining MSC power reference, we can consider following relationship between power references.

$$P^*_{MSC} + P^*_{ESS} = P^*_{GSC}, \tag{13}$$

where P^*_{MSC} and P^*_{ESS} are the MSC power reference and ESS discharge power reference, respectively. The reserve power of the ESS can be obtained by using the SoC value and fault time duration. The fault time duration is determined according to the grid codes corresponding to voltage sag. The reserve energy capacity of rotor inertia, E^{WT}_{res} can be defined by using following equation.

$$E^{WT}_{res} = \frac{1}{2}J(\omega^2_{m,max} - \omega^2_{m,del}), \tag{14}$$

E^{WT}_{res} is defined from the rotor inertia, J, and the rotor speed in de-loaded operation, $\omega_{m,del}$. To evaluate the required reserve energy and corresponding $\omega_{m,del}$, we considered the WT mechanical power production using MPPT power at a given wind speed.

$$E^{WT}_{mech} = \int_{t_s}^{t_c} P_{MPPT}\,dt, \tag{15}$$

where, t_s and t_c denote the times when the grid fault starts and clears, respectively. By considering the mechanical power production of a WT as described above, more power reserve can be prepared with de-loaded operation. That is, E^{WT}_{res} is the reserve energy which can be stored in the inertia as a kinetic energy when reducing the MSC power output and E^{WT}_{mech} is the mechanical energy when the WPS operates in the MPPT control. The mechanical energy can be transferred to the grid through the MSC or stored in inertia as the kinetic energy. To ensure stable operation of WPS during a grid voltage fault, we defined the required reserve energy (from WPS) by considering mechanical energy when the WPS operates in the MPPT control which is higher than actual mechanical power produced from WPS during LVRT. Therefore, there is sufficient reserve energy margin from the proposed method to ensure the stable operation of WPS during the grid fault. Using above energy production during a grid fault, E^{WT}_{mech}, we can obtain the rotor speed reference for proper de-loaded operation.

$$E^{WT}_{mech} - E_{ESS} = E^{WT}_{res}, \tag{16}$$

where, E_{ESS} is reserve (charging) energy considering SoC value at the time of a grid fault. Thus, we can obtain the rotor speed for the de-loaded operation.

$$\omega_{m,del} = \sqrt{\frac{2(E^{WT}_{mech} - E_{ESS})}{J\omega^2_{m,max}}} \tag{17}$$

Thus, the de-loaded operation corresponding to $\omega_{m,del}$ is determined according to the wind speed and ESS SoC. When the $E^{WT}_{mech} - E_{ESS} \leq 0$, for example, there is no need for de-loaded operation from WPS and it operates in MPPT operation without the loss of power reduction. From the proposed method, a proper de-loaded operation can be achieved considering ESS SoC status. Since ESS can be controlled for DC link voltage regulation, the ESS control algorithm could be simple and have more freedom in its operation. Therefore, ESS can be used for various grid support applications with less restriction in its SoC management. Thus, the ESS power reference and WT MSC power reference are can be obtained as following equations.

$$P^*_{ESS} = \frac{E_{ESS}}{t_c - t_s}, \tag{18}$$

$$P^*_{MSC} = \frac{E^{WT}_{res}}{t_c - t_s}, \tag{19}$$

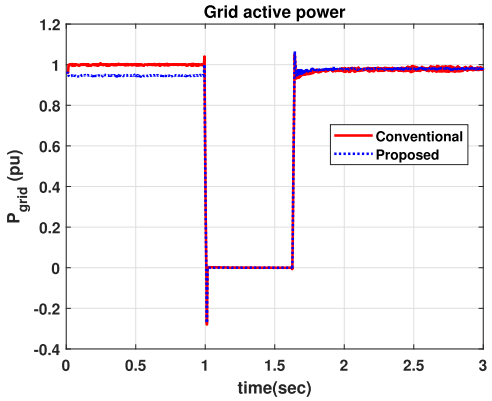

FIGURE 3. Grid active power during a balanced voltage sag (80%) using conventional LVRT method.

TABLE 1. System parameters used in simulation.

Parameter	Value	Unit
Rated power	1.63	MW
Rated wind speed	12	m/s
Rated rotor speed	10	rpm
Max. power coefficient	0.5	
Optimal tip speed ratio	9.9495	
Blade radius	33.05	m
Air density	1.12	kg/m^3
Max. rotor speed	4.335	rad/s
DC-link voltage	1150	V
Turbine inertia	6500	kgm^2
ESS capacity	1	kWh

IV. SIMULATION RESULTS

We considered a grid fault condition in case of 80% grid voltage sag. It is significant impact in LVRT operation since GSC should reduce its active power to zero and produce full reactive current during the grid fault according to the grid code. We considered two case studies. Firstly, we compared the results of the conventional LVRT method and the proposed LVRT method. In conventional method, WT is controlled for MPPT during normal state and both WT and ESS are controlled for the LVRT during grid fault. Next, we considered the different SoC condition at the time of the grid fault. As described previous section, the proposed de-loaded LVRT operation is determined according to SoC status for reliable LVRT operation. When ESS has enough reserve energy for LVRT operation, WT can be controlled as MPPT operation. We used MATLAB/Simulink SimPowerSystems toolbox for the LVRT simulation. From the simulation results, we validated the reliable operation of the proposed method considering rotor speed limit and SoC management.

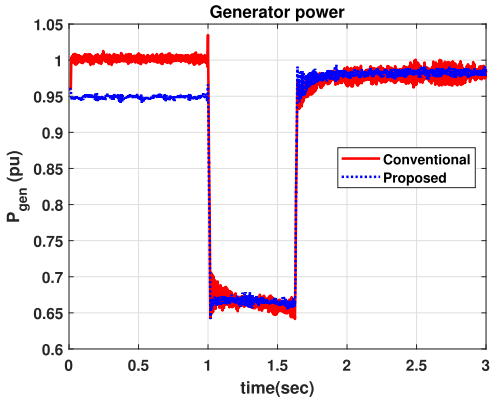

FIGURE 4. Generator active power during a balanced voltage sag (80%) using conventional LVRT method.

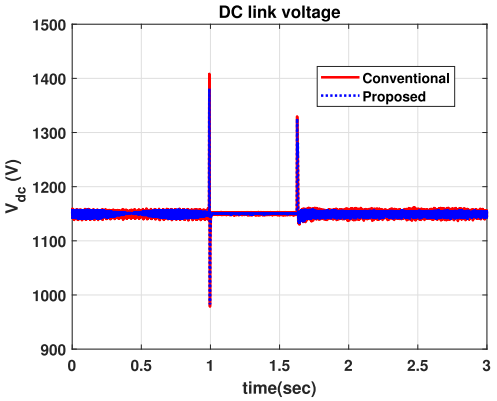

FIGURE 5. DC-link voltage during a balanced voltage sag (80%) using conventional LVRT method.

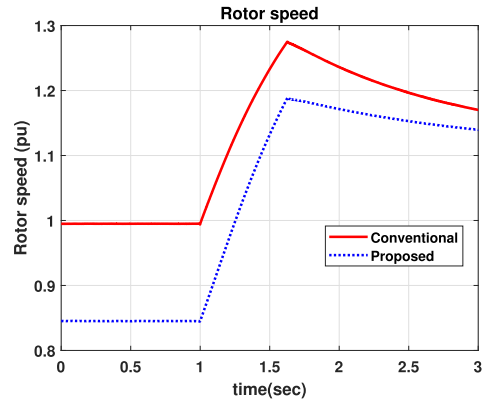

FIGURE 6. Rotor speed variation during a balanced voltage sag (80%) using conventional LVRT method.

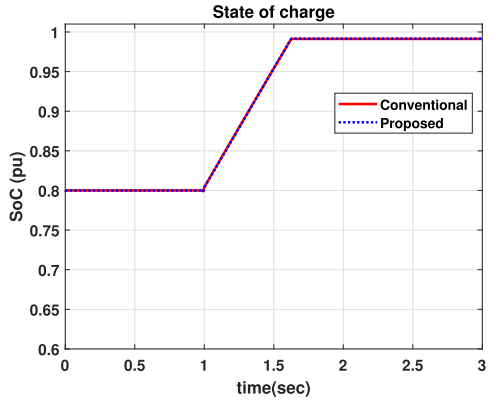

FIGURE 7. SoC during a balanced voltage sag (80%) using conventional LVRT method.

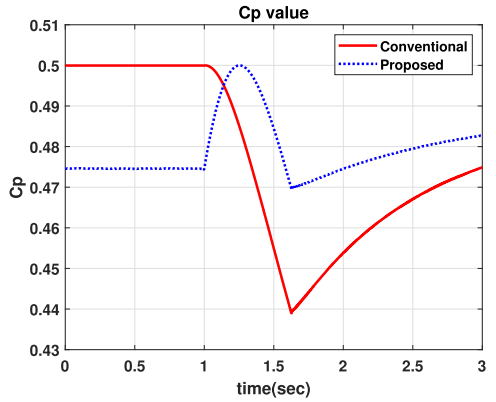

FIGURE 8. Power coefficient during a balanced voltage sag (80%) using conventional LVRT method.

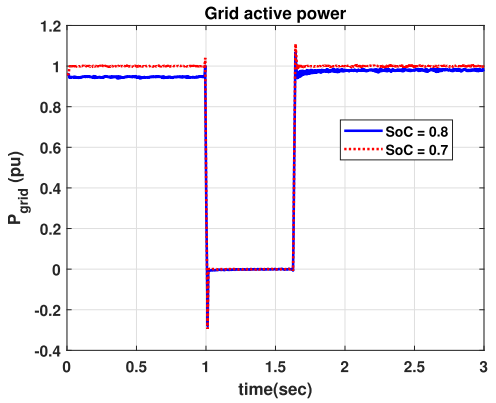

FIGURE 9. Grid active power during a balanced voltage sag (80%).

A. COMPARISON OF LVRT PERFORMANCE

Previous studies focus on the LVRT control for better dc link voltage regulation. ESS is also used for LVRT method since ESS is connected to WT for various objectives. Both WT and ESS can be coordinately controlled for better LVRT operation. However, it is needed to prepare the LVRT operation before the grid fault occurs for reliable operation of a WT. Figures from 3 to 8 shows the comparison of LVRT performance during the grid fault. Figure 3 shows grid active powers of both methods. In both methods, GSC power is zero during the grid fault. However, the proposed method reduced its power less than MPPT value considering SoC and rotor speed limit. Figure 4 shows the generator power during the grid fault. Similar to GSC power, the proposed method reduced its power which is less than MPPT value. In both methods, the powers were reduced for LVRT during the grid fault. Therefore, the proposed method has larger reserve energy capacity and can avoid the problem of unstable operation of the WPS. The proposed method obtains proper reserve capacity and finds de-loaded operation point when the Eess is less than required reserve capacity for LVRT.

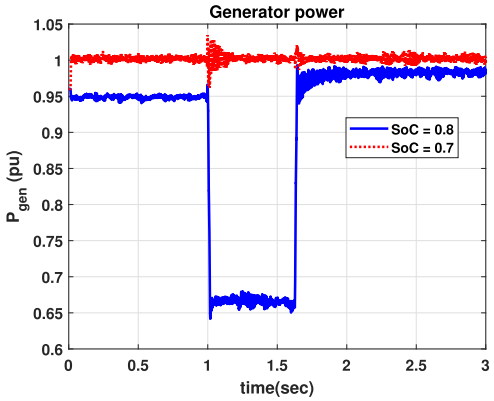

FIGURE 10. Generator active power during a balanced voltage sag (80%).

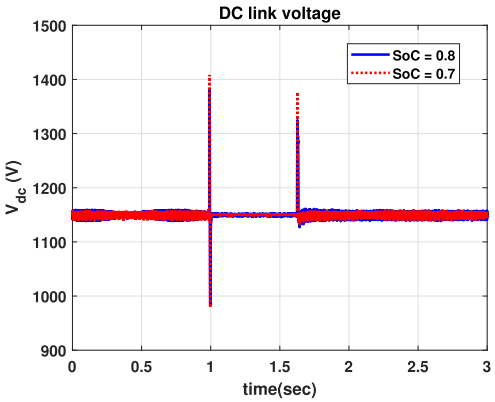

FIGURE 11. DC-link voltage during a balanced voltage sag (80%).

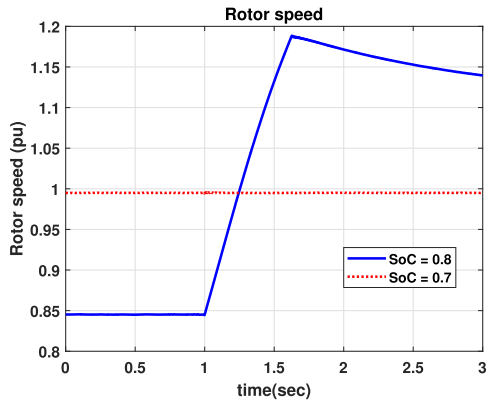

FIGURE 12. Rotor speed variation during a balanced voltage sag (80%).

Figure 5 shows the DC link voltage. both method successfully regulated the voltage during the grid fault. Figure 6 shows the rotor speed response during the grid fault. Since the rotor speed limit is 1.2 pu, there was violation in the conventional method which overs maximum rotor speed limit. However, the proposed method has less value without violating its speed limit. Figure 7 shows the SoC of the ESS during the grid fault. Both methods has similar SoC variations. If the conventional method uses more charging power reference to solve rotor speed violation, the ESS SoC could reach to one and it could result in very poor DC link regulation since SoC reach its maximum value. Figure 8 shows the WT power

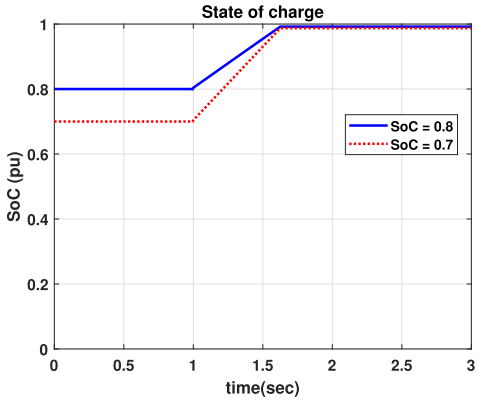

FIGURE 13. SoC during a balanced voltage sag (80%).

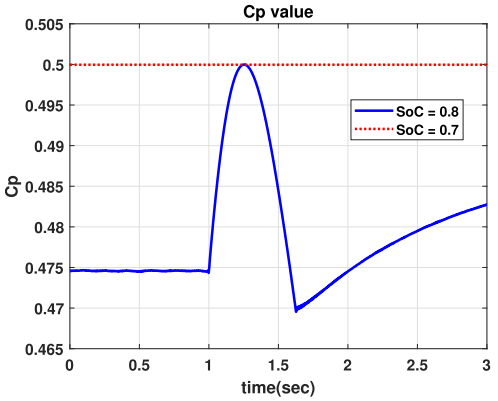

FIGURE 14. Power coefficient during a balanced voltage sag (80%).

coefficient value during the grid fault. Conventional method had maximum value as 0.5 before the grid fault occurred. In the proposed method, the power coefficient was increased as the rotor speed is increased. After reaching MPPT operation point, the power coefficient was reduced as the rotor speed is increased.

B. DIFFERENT SoC VALUES

We considered the case with different SoC values. Since the de-loaded operation for the LVRT is controlled according to SoC value, the de-loaded operation is different with given SoC value. Thus, we compared the response of the proposed method with different SoC values as 0.7 and 0.8. Figure 9 shows that the grid active powers. When the SoC is 0.7, the GSC power was MPPT value. It means that the ESS can afford whole LVRT burden. Figure 10 shows that the generator powers. Since the ESS reserve can afford whole LVRT burden, generator produce the WT MPPT value even during the grid fault. When the SoC is 0.8, however, WT was controlled in de-loaded operation and it reduced its power during the grid fault. Figure 11 shows the DC link voltages and both cases had similar responses. Figure 12 shows the rotor speeds during the grid faults. Unlike to previous results, rotor speed is remained in MPPT point when the SoC is 0.7. Figure 13 shows the SoC values during the grid fault. When the SoC is 0.7, the ESS charged more power and took more burden for the LVRT operation. In both cases, the SoC

values are less than the maximum value. Figure 14 shows the power coefficient value of the WT. When the SoC is 0.7, the power coefficient value was remained in the maximum value according to the rotor speed response. According to equation 16, The references of both WT and ESS output powers are determined. Therefore, both cases had different response according to the ESS SoC values. When the ESS has enough charging reserve energy, WT can produce maximum power during grid fault. However, both cases showed that the proposed method can effectively control the WT operation considering the ESS SoC for the reliable operation for the LVRT.

V. CONCLUSION

We proposed a de-loaded operation method for LVRT for solving reserve energy limitation problem during grid fault. We analyzed power characteristics of WPS and defined proper de-loaded operation by reducing power production from WPS. From the proposed method, the successful LVRT response is guaranteed and simulation results showed the effectiveness of the proposed method. Moreover, the amount of power reduction is minimized from the proposed method by analyzing WP characteristic. In simulation results, we validated the effectiveness of the proposed method in different fault conditions. The proposed method can be extended to further integration issues about WPS integration. As a future work, we will further research on the scheduling of the WPS and the ESS by considering both economic dispatch and LVRT. we will consider the ESS lifecycle as a cost function in scheduling problem by considering the impact of charging and discharging profile on the ESS lifecycle. Furthermore, we will study about these issues through experimental implementation and analyze the transient response under unbalanced fault.

REFERENCES

[1] H. Polinder, F. F. A. Van Der Pijl, G.-J. De Vilder, and P. J. Tavner, "Comparison of direct-drive and geared generator concepts for wind turbines," *IEEE Trans. Energy Convers.*, vol. 21, no. 3, pp. 725–733, Sep. 2006.
[2] M. Chinchilla, S. Arnaltes, and J. C. Burgos, "Control of permanent-magnet generators applied to variable-speed wind-energy systems connected to the grid," *IEEE Trans. Energy Convers.*, vol. 21, no. 1, pp. 130–135, Mar. 2006.
[3] C. Kim, Y. Gui, and C. C. Chung, "Maximum power point tracking of a wind power plant with predictive gradient ascent method," *IEEE Trans. Sustain. Energy*, vol. 8, no. 2, pp. 685–694, Apr. 2017.
[4] J. Kim, E. Muljadi, V. Gevorgian, and A. F. Hoke, "Dynamic capabilities of an energy storage-embedded DFIG system," *IEEE Trans. Ind. Appl.*, vol. 55, no. 4, pp. 4124–4134, Jul. 2019.
[5] C. Kim, E. Muljadi, and C. Chung, "Coordinated control of wind turbine and energy storage system for reducing wind power fluctuation," *Energies*, vol. 11, no. 1, p. 52, Dec. 2017.
[6] M. Tsili and S. Papathanassiou, "A review of grid code technical requirements for wind farms," *IET Renew. Power Gener.*, vol. 3, no. 3, pp. 308–332, 2009.
[7] G. Saccomando, J. Svensson, and A. Sannino, "Improving voltage disturbance rejection for variable-speed wind turbines," *IEEE Trans. Energy Convers.*, vol. 17, no. 3, pp. 422–428, Sep. 2002.
[8] A. Mullane, G. Lightbody, and R. Yacamini, "Wind-turbine fault ride-through enhancement," *IEEE Trans. Power Syst.*, vol. 20, no. 4, pp. 1929–1937, Nov. 2005.
[9] J. Matas, M. Castilla, J. M. Guerrero, L. G. de Vicuna, and J. Miret, "Feedback linearization of direct-drive synchronous wind-turbines via a sliding mode approach," *IEEE Trans. Power Electron.*, vol. 23, no. 3, pp. 1093–1103, May 2008.
[10] J. F. Conroy and R. Watson, "Low-voltage ride-through of a full converter wind turbine with permanent magnet generator," *IET Renew. Power Gener.*, vol. 1, no. 3, pp. 182–189, Sep. 2007.
[11] K.-H. Kim, Y.-C. Jeung, D.-C. Lee, and H.-G. Kim, "LVRT scheme of PMSG wind power systems based on feedback linearization," *IEEE Trans. Power Electron.*, vol. 27, no. 5, pp. 2376–2384, May 2012.
[12] S. Alepuz, A. Calle, S. Busquets-Monge, S. Kouro, and B. Wu, "Use of stored energy in PMSG rotor inertia for low-voltage ride-through in back-to-back NPC converter-based wind power systems," *IEEE Trans. Ind. Electron.*, vol. 60, no. 5, pp. 1787–1796, May 2013.
[13] H. Geng, C. Liu, and G. Yang, "LVRT capability of DFIG-based WECS under asymmetrical grid fault condition," *IEEE Trans. Ind. Electron.*, vol. 60, no. 6, pp. 2495–2509, Jun. 2013.
[14] W. Wang, B. Ge, D. Bi, M. Qin, and W. Liu, "Energy storage based LVRT and stabilizing power control for direct-drive wind power system," in *Proc. Int. Conf. Power Syst. Technol.*, Oct. 2010, pp. 1–6.
[15] J. Liu, W. Yao, J. Fang, J. Wen, and S. Cheng, "Stability analysis and energy storage-based solution of wind farm during low voltage ride through," *Int. J. Electr. Power Energy Syst.*, vol. 101, pp. 75–84, Oct. 2018.
[16] J. Yao, J. Li, L. Guo, R. Liu, and D. Xu, "Coordinated control of a hybrid wind farm with PMSG and FSIG during asymmetrical grid fault," *Int. J. Electr. Power Energy Syst.*, vol. 95, pp. 287–300, Feb. 2018.
[17] J. Li, N. Wang, D. Zhou, W. Hu, Q. Huang, Z. Chen, and F. Blaabjerg, "Optimal reactive power dispatch of permanent magnet synchronous generator-based wind farm considering levelised production cost minimisation," *Renew. Energy*, vol. 145, pp. 1–12, Jan. 2020.
[18] C. Kim and W. Kim, "Enhanced low-voltage ride-through coordinated control for PMSG wind turbines and energy storage systems considering pitch and inertia response," *IEEE Access*, vol. 8, pp. 212557–212567, 2020.
[19] M. E. Haque, M. Negnevitsky, and K. M. Muttaqi, "A novel control strategy for a variable speed wind turbine with a permanent magnet synchronous generator," in *Proc. IEEE Ind. Appl. Soc. Annu. Meeting*, Oct. 2008, pp. 1–8.

CHUNGHUN KIM (Member, IEEE) received the B.S. degree in electronic electricity computer engineering from Hanyang University, Seoul, South Korea, in 2011, and the unified M.S. and Ph.D. degrees in electrical engineering from Hanyang University, in 2018. In 2017, he was a Visiting Scholar with the National Renewable Energy Laboratory, Colorado, USA. In 2018, he was a Postdoctoral Researcher with the Department of Electrical Engineering, Kyungpook National University, Deagu, South Korea, where he worked as a Research Professor, in 2019. He is currently an Assistant Professor with the Department of AI Electrical Engineering, Pai Chai University, Daejeon, South Korea. His current research interests include integration of renewable energy and optimization of distributed energy resource in micro-grid.

WONHEE KIM (Member, IEEE) received the B.S. and M.S. degrees in electrical and computer engineering and the Ph.D. degree in electrical engineering from Hanyang University, Seoul, South Korea, in 2003, 2005, and 2012, respectively. From 2005 to 2007, he was with Samsung Electronics Company, Suwon, South Korea. In 2012, he was with the Power and Industrial Systems Research and Development Center, Hyosung Corporation, Seoul. In 2013, he was a Postdoctoral Researcher with the Institute of Nano Science and Technology, Hanyang University, and a Visiting Scholar with the Department of Mechanical Engineering, University of California, Berkeley, CA, USA. From 2014 to 2016, he was with the Department of Electrical Engineering, Dong-A University, Busan, South Korea. He is currently an Associate Professor with the School of Energy Systems Engineering, Chung-Ang University, Seoul. His current research interests include nonlinear control and nonlinear observers, as well as their industrial applications. He has served as an Associate Editor for IEEE Access and the *Journal of Electrical Engineering and Technology*.